# Chapter 8
# Toolbox for Applied Seismic Tomography (TOAST)

**Thomas Forbriger, Michael Auras, Filiz Bilgili, Thomas Bohlen, Simone Butzer, Sandra Christen, Luigia Cristiano, Wolfgang Friederich, Rüdiger Giese, Lisa Groos, Heiner Igel, Florian Köllner, Rolf Krompholz, Stefan Lüth, Stefan Mauerberger, Thomas Meier, Ilaria Mosca, Dirk Niehoff, Heike Richter, Martin Schäfer, Andreas Schuck, Florian Schumacher, Karin Sigloch, Mario Vormbaum and Frank Wuttke**

**Abstract** TOAST (Toolbox for Applied Seismic Tomography) makes methods of full-waveform inversion of elastic waves available for the practitioner. The inversion of complete seismograms is an utmost ambitious and powerful technology. One of its strengths is the enormously increased imaging-resolution since it is able to resolve structures smaller than the seismic wave length. Further it is sensitive to material properties like density and dissipation which are hardly accessible through

T. Forbriger (✉) · T. Bohlen · S. Butzer · L. Groos · M. Schäfer
Karlsruhe Institute of Technology (KIT), Karlsruhe, Germany
e-mail: thomas.forbriger@kit.edu

M. Auras
Institut für Steinkonservierung e.V. Mainz, Mainz, Germany

F. Bilgili · S. Christen · L. Cristiano · T. Meier · F. Wuttke
Christian-Albrechts-Universität zu Kiel (CAU), Kiel, Germany

W. Friederich · F. Schumacher
Ruhr-University Bochum (RUB), Bochum, Germany

R. Giese · S. Lüth · H. Richter
Helmholtz Centre Potsdam (GFZ), Potsdam, Germany

H. Igel · S. Mauerberger · I. Mosca · K. Sigloch
Ludwig-Maximilians-University (LMU), Munich, Germany

F. Köllner · A. Schuck · M. Vormbaum
Geophysik und Geotechnik Leipzig GmbH (GGL), Leipzig, Germany

R. Krompholz
Geotron Elektronik (GEOTRON), Pirna, Germany

D. Niehoff
Dornburger Zement GmbH and Co. KG, Dorndorf-Steudnitz, Germany

M. Weber and U. Münch (eds.), *Tomography of the Earth's Crust: From Geophysical Sounding to Real-Time Monitoring*, Advanced Technologies in Earth Sciences,
DOI: 10.1007/978-3-319-04205-3_8, 

conventional techniques. Within the TOAST project algorithms available in academia were collected, improved, and prepared for application to field recordings. Different inversion strategies were implemented (global search, conjugate gradient, waveform sensitivity kernels) and computer programs for imaging the subsurface in 1D, 2D, and 3D were developed. The underlying algorithms for the correct numerical simulation of physical wave propagation have thoroughly been tested for artefacts. In parallel these techniques were tested in application to waveform data. They proved their potential in application to synthetic data, shallow-seismic surface waves from field recordings, and microseismic and ultrasonic data from material testing. This provided valuable insight to the demands on seismic observation equipment (repeatability, waveform reproduction, survey layout) and inversion strategies (initial models, regularization, alternative misfit definitions, etc.). The developed software programs, results of benchmark tests, and field-cases are published online by the OpenTOAST.de initiative.

## 8.1 Introduction

Full-waveform inversion (FWI) is a leading edge technique to exploit the full signal content of seismic data. It promises sub-wavelength resolution, high performance in resolving P- and S-wave velocity as well as sensitivity to variations in mass density. In particular for surface wave studies, where conventional methods require lateral homogeneity of the structure under investigation, FWI opens a new window to subsurface imaging. The computational demands for FWI are extraordinary and require state-of-the-art equipment and large computer clusters in the case of 3D application. Meanwhile a variety of implementations are developed in academic environments. Their potential is mainly demonstrated on synthetic data. The TOAST project pursues the goal to make these implementations available to a broader community as well as to end-users.

We established a unique knowledge base through a fertile collaboration of universities (Karlsruhe Institute of Technology [KIT], Ruhr-University Bochum [RUB], Christian-Albrechts-Universität zu Kiel [CAU], and Ludwig-Maximilians-University Munich [LMU]), the Helmholtz Centre Potsdam (GFZ), and commercial companies (Geophysik und Geotechnik Leipzig GmbH [GGL] and Geotron Elektronik [GEOTRON]). Contributions from wave propagation and inverse theory, numerical programming, IT management, field experience in shallow-seismics as well as ultrasonics and microseismics on application targets were successfully brought together.

In the current contribution we present some selected results of the joint project. We feature three different approaches to FWI. The adjoint method currently is a widespread approach, since it is of outstanding numerical efficiency. The computation of waveform kernels is much more demanding but offers improved convergence and the potential for resolution analysis. If the parameter space for subsurface models can be kept small, as is the case in material testing, global search algorithms can explore the

full non-uniqueness of the inverse problem. The aim of TOAST is not only to demonstrate the fitness of these approaches by application to synthetic data. We long for the successful inversion of field data. In field laboratories on the shallow-seismic and the ultrasonic (material testing) scale we recorded waveform data. The field laboratories not only produced challenges for the FWI but also many insights in properties of seismic sources (partly developed within the project), appropriate surveying and new insights to seismic properties of the different materials under investigation. The final products of the project in terms of computer code, benchmark data, technical definitions, and recommendations we share with a broader community through the web portal OpenTOAST (http://www.opentoast.de). A prerequisite for this is the resolution of licensing issues and basic documentation. The TOAST members hope that this initiative will remain prosperous after the end of the funding period.

The scientific results of the joint project go beyond this brief contribution. They will be published in separate research papers within the near future (Butzer et al. 2013; Forbriger et al. submitted; Groos et al. in prep; Krauss et al. submitted; Kurzmann et al. 2013; Mosca et al. submitted; Schäfer et al. submitted). Three dissertations use TOAST software for the FWI of reflected acoustic waves (Kurzmann 2012; Przebindowska 2013) as well as surface waves (Groos 2013). Further disserations are in preparation in the context of TOAST.

## 8.2 Full-Waveform Inversion with the Adjoint Method

Full-waveform inversion (FWI) aims to minimize the misfit between modeled and observed seismograms. This can be implemented efficiently using a conjugate gradient approach (Tarantola 1988; Mora 1987). The adjoint-state method enables to calculate the gradient of the misfit function as zero-lag cross-correlation between a forward propagated wavefield and a wavefield propagated back from the receivers into the medium. Hereby the explicit calculation of the Fréchet derivatives can be avoided.

We use the time-domain 2D elastic FWI code developed by Köhn (2011), which is available under the terms of GNU GPL at http://www.opentoast.de. For the inversion of shallow-seismic field data this code was further enhanced by implementing different misfit definitions, source wavelet inversion and viscoelasticity.

Time domain FWI requires the storage of wavefields of the whole time series for gradient calculations. By contrast, in the frequency domain only few discrete frequencies can be sufficient for the gradient calculations, known as single frequency inversion (Sirgue and Pratt 2004). As the wavefield needs to be stored only for these frequencies, storage costs decrease dramatically. In our 3D FWI implementation we therefore adopted the approach suggested by Sirgue et al. (2008). This is a combination of forward modeling in the time domain and inversion in the frequency domain and offers an optimal approach to minimize storage needs and runtime. Using discrete Fourier transformations the wavefields can be transformed from time into frequency domain on the fly. The gradients are then calculated as multiplications of forward and

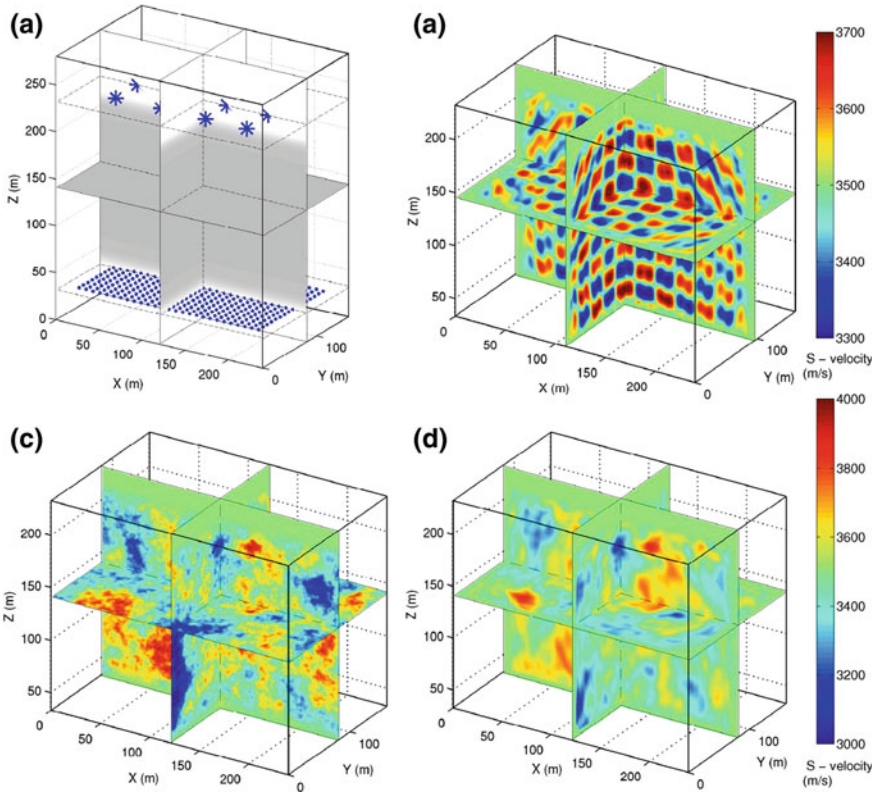


**Fig. 8.1** Inversion results of 3D FWI for S-velocity: **a** 3D acquisition geometry with sources (∗) and receivers (+), **b** inversion result checkerboard (±5 % variation), **c** real model random medium and **d** random medium inversion result

conjugate backpropagated wavefields in the frequency domain. This approach additionally enables to increase the frequency during inversion without further effort. Starting from sufficiently low frequencies is extremely important to decrease the ambiguity of the inverse problem (e.g. Sirgue and Pratt 2004).

The modeling of two and three-dimensional wavefields is performed with a time-domain elastic finite-difference code based on the velocity stress formulation on a staggered grid (Bohlen 2002). The code is heavily parallelized and thus enables a very efficient and fast calculation of the wavefields.

### *8.2.1 3D Elastic Full-Waveform Inversion*

Here we present two inversion tests for $v_p$ and $v_s$ using homogeneous starting models with $v_p = 6300\,\mathrm{m/s}$, $v_s = 3500\,\mathrm{m/s}$ and $\rho = 2800\,\mathrm{kg/m^3}$. Figure 8.1 shows results

for $v_s$ only. The inverted P-wave velocity models are much smoother due to their larger wavelengths. Figure 8.1a shows the acquisition geometry, consisting of 12 sources and 416 receivers in transmission geometry.

A resolution study was performed, using a checkerboard with 5 % velocity variation and 20 m edge length. Frequencies were increased from 140 to 240 Hz. The result is shown in Fig. 8.1b. The alternating cubes are well reconstructed, except at the boundaries. The sharp contrast between the cubes could not be resolved and requires the use of higher frequencies.

In a second inversion test, we inverted data of a random medium model, described by an exponential autocorrelation function in space. The real shear wave velocity model is plotted in Fig. 8.1c. The model represents a crystalline rock environment. The S-velocity result is shown in Fig. 8.1d. The inversion method could successfully recover the differently sized 3D random medium structures down to the scale of a wavelength. Higher frequencies would be required to reconstruct smaller features. Similar to the resolution test, we find that the resolution of the result decreases towards model boundaries, where wavepath coverage is less.

### *8.2.2 2D Elastic Full-Waveform Inversion*

We apply a 2D FWI to shallow-seismic Rayleigh waves. Shallow-seismic Rayleigh waves can be easily excited by a hammer blow on the surface and have a high sensitivity to the shear wave velocity in the first meters of the subsurface. We apply FWI to a field dataset acquired on a test site of the TOAST field laboratory at Rheinstetten near Karlsruhe (Germany). The subsurface consists of layered fluviatile sediments. Figure 8.2 displays the inversion results. The data misfit is significantly decreased during the inversion. Furthermore, the S-wave velocity model still corresponds to a predominantly depth dependent structure even though this is not enforced in the inversion by regularization. Although the changes in the S-wave velocity model are small, these changes have a strong influence on the wavefields which confirms the high sensitivity of Rayleigh waves to the S-wave velocity model of the shallow subsurface.

## 8.3 Full-Waveform Inversion and Sensitivity Analysis Using Waveform Sensitivity Kernels

We derive waveform sensitivity kernels from Born scattering theory, for use in an iterative full-waveform inversion procedure that tries to explain the full information content of measured seismic waveforms by inhomogeneities of the structural elastic earth model. Additionally, the sensitivity kernels may be used to follow various strategies of seismic sensitivity and resolution analysis.

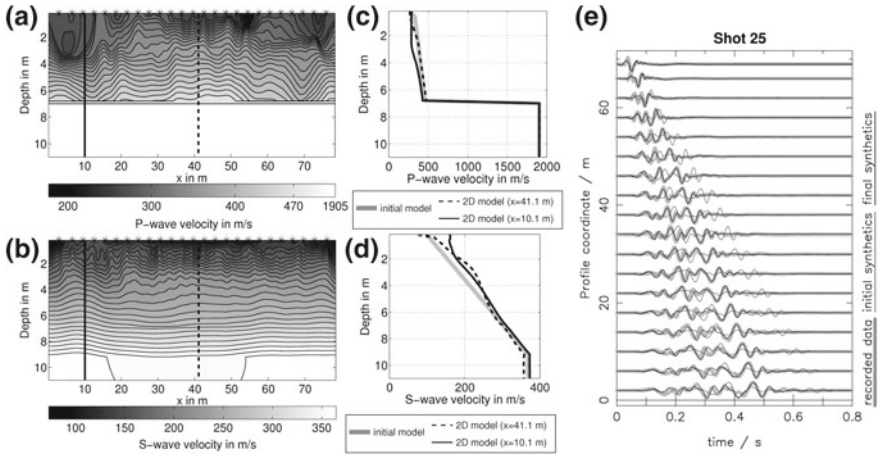


**Fig. 8.2** 2D subsurface model obtained by FWI. **a** displays the P-wave velocity model and **b** the S-wave velocity model. The stars mark the source positions. **c** and **d** shows the corresponding vertical velocity profiles in comparison to the initial model. **e** displays vertical displacement seismograms for shot 25 (x = 77.0 m) in the frequency band between 5 and 70 Hz. Recorded data are displayed by the thick gray line, seismograms calculated with the initial model are displayed by the thin gray line and seismograms calculated with the 2D model are displayed in black. Each trace is normalized to its maximum amplitude

### *8.3.1 Waveform Sensitivity Kernels*

In the context of Born scattering, we may derive the following expression of the scattered displacement field $\delta\mathbf{u}$, starting of with the elastodynamic equation in the frequency domain and using Betti's theorem and the reciprocity property of Green functions

$$\delta u_n(\mathbf{r}) = \int_\Omega \Big[\delta\rho G_{in}(\mathbf{r}_s, \mathbf{r})\,\omega^2 u_i(\mathbf{r}_s) - \delta c_{ijkl}\partial_j G_{in}(\mathbf{r}_s, \mathbf{r})\,\partial_l u_k(\mathbf{r}_s)\Big] d^3\mathbf{r}_s \quad (8.1)$$

where $G_{in}(\mathbf{r}_s, \mathbf{r})$ denotes the $i^{\text{th}}$ displacement component at $\mathbf{r}_s$ for a delta force in $n$-direction at $\mathbf{r}$, $\rho$ and $c_{ijkl}$ denote density and tensor of linear elasticity and leading $\delta$ indicates the perturbed/scattered property. Einstein summation convention is assumed and integration is done over the whole volume of interest $\Omega$, where perturbed boundaries, hence contributions by surface integrals, are omitted.

For a specific linear elastic parametrization of $N$ parameters $p_1, \ldots, p_N$, the integrand in Eq. (8.1) may be linearly rearranged to yield

$$\delta u_n(\mathbf{r}) = \int_\Omega \Big[\delta p_1 K_{n\mathbf{r}}^{p1}(\mathbf{r}_s) + \cdots + \delta p_N K_{n\mathbf{r}}^{p_N}(\mathbf{r}_s)\Big] d^3\mathbf{r}_s, \quad (8.2)$$

where the frequency dependent expressions $K_{n\mathbf{r}}^{p_j}(\mathbf{r}_s)$ quantify how the $n^{\text{th}}$ component $u_n(\mathbf{r})$ of the displacement spectrum at receiver position $\mathbf{r}$ changes, if model parameter $p_j$ is perturbed by $\delta p_j$ at scattering point $\mathbf{r}_s$ inside the medium. Hence, we call quantities $K$ *waveform sensitivity kernels*, which by symmetries of tensor $c_{ijkl}$ may be expressed in terms of displacement field $\mathbf{u}$, Green tensor $\mathbf{G}$ and their strains, respectively.

### 8.3.2 Software Package ASKI

We developed and implemented the highly modularized software package ASKI—Analysis of Sensitivity and Waveform Inversion—which applies the scattering relation (8.2) to a specific choice of model parameters $p_j$ (e.g. $p_j \in \{\rho, \lambda, \mu\}$, or $p_j \in \{\rho, v_p, v_s\}$). For these parameters, ASKI computes the waveform sensitivity kernels $K$ from synthetic displacement fields, Green tensors and their strains which are calculated by a supported forward method w.r.t. some (possibly already heterogeneous) background model and stored in the frequency domain throughout $\Omega$.

At the moment the 3D spectral element code SPECFEM3D (Tromp et al. 2008) and the1D semi-analytical code GEMINI (Friederich and Dalkolmo 1995) in both, Cartesian and spherical framework are supported. ASKI can be easily extended to other forward methods.

ASKI discretizes the model space into values $p_{js}$ of the elastic parameters $p_j$ on a set of scatterers $\Omega_s$, which are a disjoint division of the model domain $\Omega$. This way, (8.2) leads to the linear relation

$$\delta u_n(\mathbf{r}) = \sum_s \left[ \delta p_{1s} \int_{\Omega s} K_{n\mathbf{r}}^{p1} + \cdots + \delta p_{Ns} \int_{\Omega s} \mathrm{K}_{n\mathbf{r}}^{p_N} \right], \tag{8.3}$$

assuming the parameter perturbations $\delta p_{js}$ to be constant throughout scatterer $\Omega_s$.

Using the linear relation (8.3), possibly setting up a linear system of equations for many data, various strategies of sensitivity and resolution analysis, as well as an iterative full-waveform inversion procedure may be followed, as presented in the following.

### 8.3.3 Iterative Full-Waveform Inversion

The waveform sensitivity kernels can be used to invert structural earth model parameters from a given set of seismic data, taking the full content of information contained in the waveforms into account.

Starting of with some good approximation of the true earth model, we can now iteratively compute waveform sensitivity kernels w.r.t. the currently inverted model

and improve it by inferring parameter perturbations $\delta p_{js}$ from a linear system of equations, which is established by evaluating Eq. (8.3) on a set of data. The scattered wavefield $\delta u_n$ (**r**) is computed as the difference of the measured data (interpreted as displacement w.r.t. the perturbed model) and synthetic displacement w.r.t. the currently inverted model.

In order to regularize the inverse problem, we can use low frequency content of data for the firrst iteration steps and gradually increase the amount of waveform information to higher frequencies as we iterate. Also smoothing constraints, added as additional equations to the linear system, may help to yield sensible physical solutions.

As the steps of forward simulation, i.e. computation of synthetic wavefields, the kernel computation and the actual inversion step are kept completely separate in ASKI, the software is very flexible in terms of using different forward methods or subsets of data and varying the model resolution and intensity of smoothing.

A validation of the iterative full-waveform inversion of ASKI using waveform sensitivity kernels is shown in Fig. 8.3:

In between 12 vertical point sources at the top (yellow) and 12 3-component receivers at the bottom (red), a model inhomogeneity in $v_s$ is placed (of size 48 $\times$ 48 $\times$ 36 m), as shown in Fig. 8.3a. Simultaneously the isotropic earth model is also perturbed in $v_p$. Density is kept constant.

The homogeneous background is used as a starting model Fig. 8.3b. Figure 8.3c, d shows intermediate results of the shear-wave velocity model in the course of the iterative inversion, in which model perturbations were allowed only inside the volume of the true inhomogeneity. $v_p$ was inverted for jointly, but is not shown here.

Note that already after two iterations, the shear-wave velocity model is explained pretty well. Keep in mind, however, the unrealistic conditions of this experiment, assuming no model perturbations outside the known volume of inhomogeneity.

### *8.3.4 Sensitivity and Resolution Analysis*

As the waveform sensitivity kernels quantify how sensitive the particular data are to changes of certain model parameters, they may also be used to estimate the resolving power of a dataset and may even help in active seismic experiments to find an optimal acquisition geometry that resolves the volume of interest best, before actually collecting any data.

Any sensitivity analysis tools working on the sensitivity matrix, even a full singular value decomposition, may be easily added to ASKI using any modules provided by the ASKI program package.

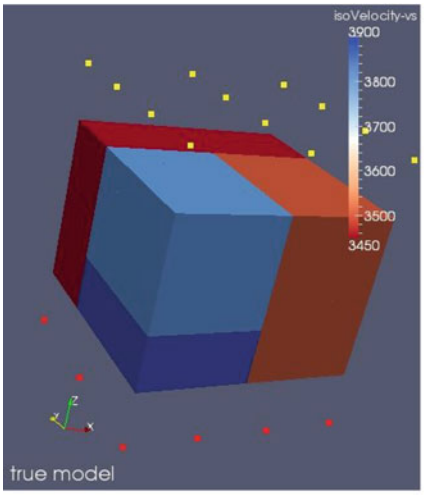


**(a)** true $v_s$ model

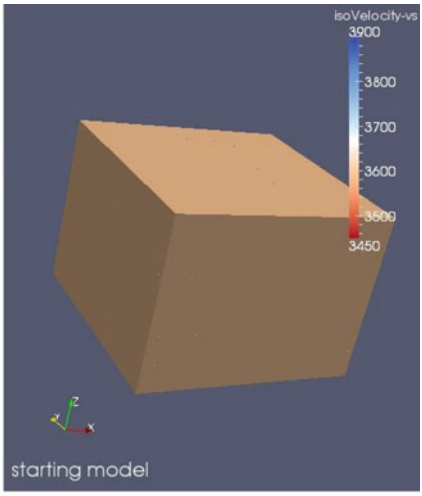


**(b)** $v_s$ starting model

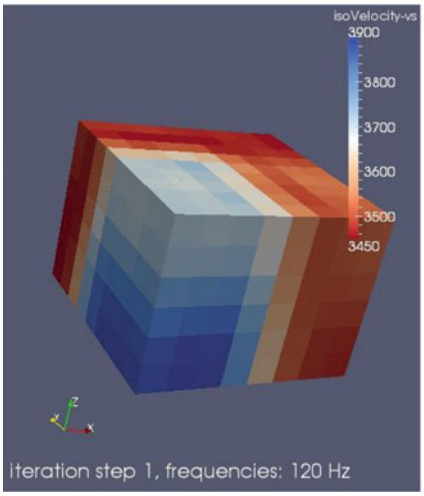


**(c)** inverted $v_s$ model after the 1st iteration

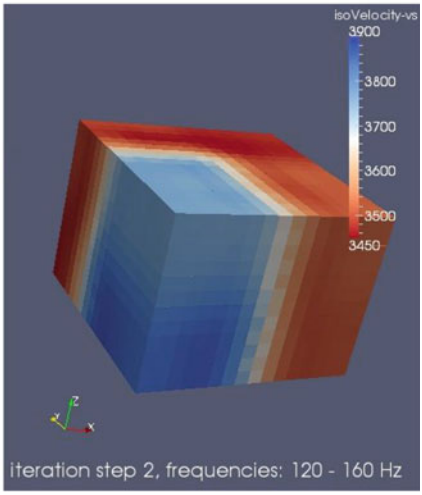


**(d)** inverted $v_s$ model after the 2nd iteration

**Fig. 8.3** Validation of ASKI full-waveform kernel inversion. Note that the frequency content of the data as well as the model resolution was increased for the 2nd iteration

## 8.4 Full-Waveform Inversion by a Global Search Algorithm Applied to Ultrasonic Data

Non-destructive testing based on ultrasounds allows us to detect, characterize and size discrete flaws in geotechnical and engineering structures and materials. This information is needed to determine whether such flaws can be tolerated in future service. In typical ultrasonic experiments, only the first-arriving P-wave is interpreted, and the remainder of the recorded waveform is neglected. Furthermore, travel-times of first arriving P-waves have limited resolution for the upper centimeters of an object. In contrast, surface measurements are well suited to quantify superficial alterations of material properties, e.g. due to weathering.

In order to characterize well a geotechnical structure, the first step is to benchmark the propagation of ultrasonic surface waves in materials tested with a non-destructive technique. The tremendous potential of ultrasonic surface waves becomes an advantage only if numerical forward modeling tools and spectral analysis are available to describe the waveforms accurately and to distinguish the contribution of surface wave modes. For this reason we compute synthetic full seismograms as well as group and phase velocity spectral analysis for certain synthetic models that resemble structures commonly tested with non-destructive technique (e.g. unweathered and weathered natural stones and concretes and road pavement). They can be end-member models for real structures analysed in field surveys. This synthetic work highlights the fact that even in seemingly simple, multi-layered structures, Rayleigh wavefields of considerable complexity develop. For this reason, not only forward modeling of synthetic seismograms but also spectral analysis of both phase and group velocity are important tools for characterizing these structures (Mosca et al. submitted).

The study of wave propagation for synthetic structures provides an useful background for setting up inverse problem formulations and therefore inferring subsurface structure from ultrasonic Rayleigh wave measurements. This will entail adopting a proper parameterization (e.g. shear wave velocity, interface thickness and shear quality factor), and efficient solvers for a generally non-linear problem. Unlike in seismological studies where reference models for layered Earth structure have been investigated extensively and are well constrained, at geotechnical scale there is often so little prior information about sub-surface properties that estimating an adequate initial model may represent the largest challenge. In the context of the TOAST project we have developed an inversion strategy based on a Monte Carlo procedure which is already modularized into the basic components of a typical inverse problem (e.g. the forward modeling, the computation of the misfit function in terms of waveform, phase or group velocity dispersion curve). Specifically, the inversion is based on the Neighborhood Algorithm (Sambridge 1999a, b) whose great advantage is the possibility to compute the appraisal problem (i.e. quantitative assessment of uncertainty and resolution) of the estimated solution(s). However, it becomes computationally expensive with increasing the number of model parameters and thus we envision it to be used mainly for estimation of layered structures. This might then serve as starting models for linearized, higher-dimensional inversions in 2D or 3D.

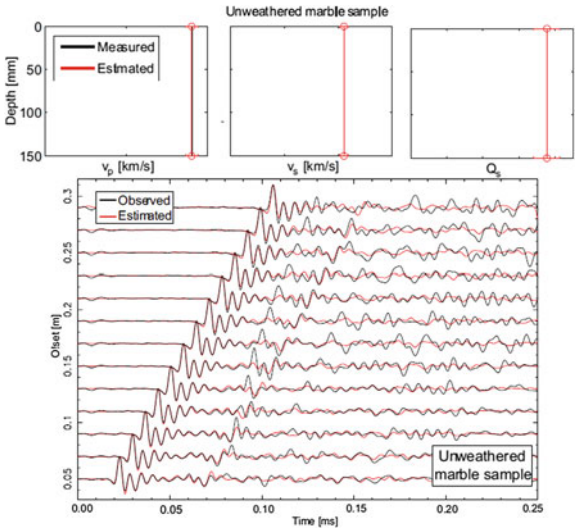


**Fig. 8.4** In the *top panel* the estimated model (compressional wave velocity, shear wave velocity and shear quality factor) is displayed together with the associated error-bars, compared with the model a priori known for unweathered marble. In the *bottom panel* seismograms computed for the estimated model and the observed seismograms are compared

We have applied successfully this inversion scheme to data from material testing, and thus defining seismic properties of models of wavelength from centimetres to meters as a function of depth. We inverted the surface-wave portion of observed seismograms for inferring the shear wave velocity, $v_s$, and the attenuation parameters, Qs, of structures. In Fig. 8.4, as an example, we show the results for ultrasonic Rayleigh wave measurements recorded at the surface of an unweathered marble sample.

To test the validity and flexibility of the scheme of our waveform inversion, we inverted also shallow-seismic measurements. An example is displayed in Fig. 8.5.

## 8.5 The Shallow-Seismic Field Laboratory

A field laboratory was set up to record data on test sites and to develop optimal acquisition strategies and quality control with respect to the subsequent full-waveform inversion (FWI). We selected a test site on the vertical fault system of the southern rim of the Taunus (near Frankfurt on the Main, Hesse, Germany). With preparatory investigations (seismics and DC geoelectrics) we confirmed the predominantly 2D nature of the subsurface. In the northwestern part of the vertical fault sericite-gneiss is met at shallow depth (0.5–2 m), while it is covered by sedimentary layers of up to 6 m thickness southeast of the fault. This is confirmed by Dynamic Probing Light (DPL) investigations and borehole profiles in the near vicinity. Perpendicular to this 2D fault we carried out a shallow-seismic 2D survey in summer of 2011. As sources we used pneumatic impulse hammer, magnetostrictive vibrator and classical hammer blows.

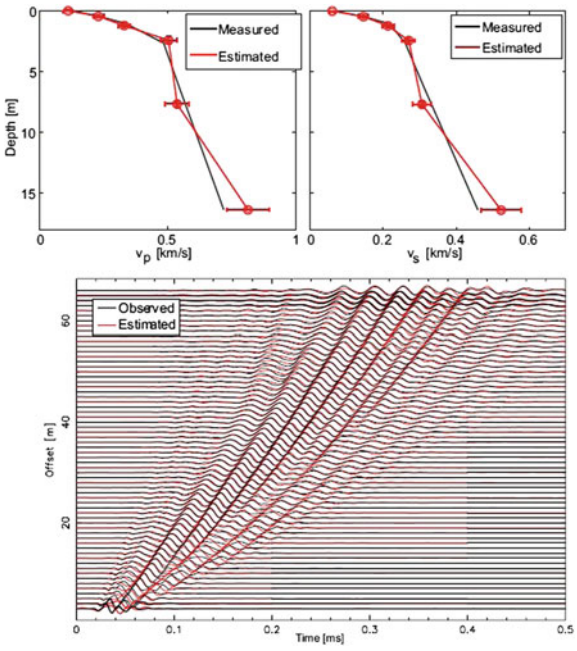


**Fig. 8.5** Like Fig. 8.4, but for the shallow-seismic survey at the site of Bietigheim. In the *top panel* the estimated compressional wave velocity, shear wave velocity and thickness of interfaces are displayed together with the known values. In the *lower panel* the synthetic data is compared with the seismograms for the inferred model

We aim to apply FWI to this field dataset. In a first step we use well established first arrival time tomographic methods. This leads to suitable initial models which are essential for successful FWI.

### *8.5.1 Performance of Different Seismic Sources*

Two mechanical seismic sources, the pneumatic impulse hammer and the magnetostrictive vibrator source, were used by GFZ to perform shallow-seismic measurements on the test site. On the vibro source, two actuators are driven synchronously with controlled and amplified frequency sweeps of same amplitude and phase. The head accelerations are detected for control of amplitudes and phases. Within the impulse hammer a pneumatically pre-stressed impact mass is unlatched from its initial position.

The data of the magnetostrictive vibrator source and the impulse hammer were acquired on the main profile. The profile length is about 89 m, with 39 vertical-geophones and 50 three-components-geophones at 1 m interval. The survey set-up of the receivers was the same for both sources. The shot points were located at the main profile at a 2 m interval for the vibrator source and 4 m for the impulse source.

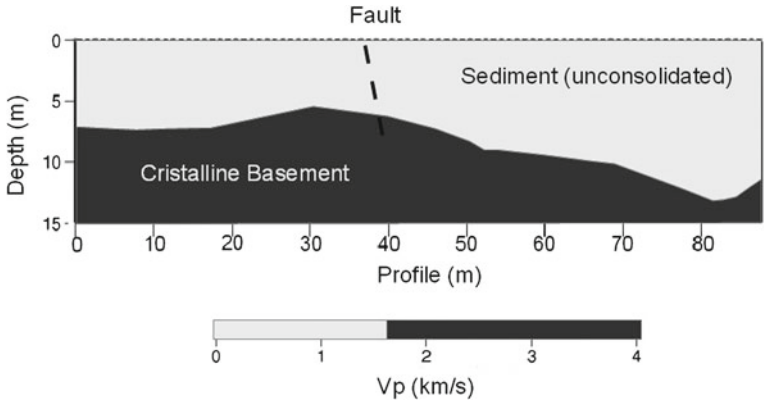


**Fig. 8.6** Velocity model as derived from tomographic inversion of the first break traveltimes picked in the data acquired using the magnetostrictive seismic source

### *8.5.2 Traveltime Tomography of Field Data*

A comparison of the data sets acquired using the pneumatic impact hammer and the magnetostrictive vibro source showed that the impact hammer data were strongly dominated by (low frequency, $<100$ Hz ) surface wave signals, whereas the vibro data were dominated by higher frequencies and a broader frequency spectrum consistent with the frequency range of the source sweep. The vibro data do not contain surface wave signals and the first breaks of the P-waves could easily be identified. Therefore, the vibro-seismic data set was used for deriving a P-wave velocity model along the acquisition profile. The traveltime tomography was performed using the FAST package by Zelt and Barton (1998). The resulting final model is shown in Fig. 8.6. The low-velocity sedimentary layer can be clearly separated from the crystalline basement layer below and the varying thickness of the sediment layer on either side of the fault zone in the middle of the profile can be identified.

Vertical and horizontal hammer blows were used to obtain shallow-seismic data at Mammolshain for the inversion of P- and S-wave travel-times. Due to small receiver and shotpoint spacings the geometry of the main seismic profile is suitable for the application of traveltime tomography, which estimates the 2D velocity distribution along the profile. Starting velocity models are separately generated based on this inversion process for P- and S-wave first arrivals. The software Rayfract® (Seismic Refraction and Borehole Tomography) uses a 1D gradient initial model which is directly determined from first breaks and further invokes an iterative refinement of this initial 1D velocity model with a 2D WET (Wavepath Eikonal Traveltime) inversion code. This inversion code is based on a finite-difference solution to the Eikonal equation. Traveltimes are corrected for topography and the inversion process is terminated after 20 iterations. The inferred velocity models are displayed in Fig. 8.7. The stratigraphy is simplified by two different colors: The upper light gray repre-

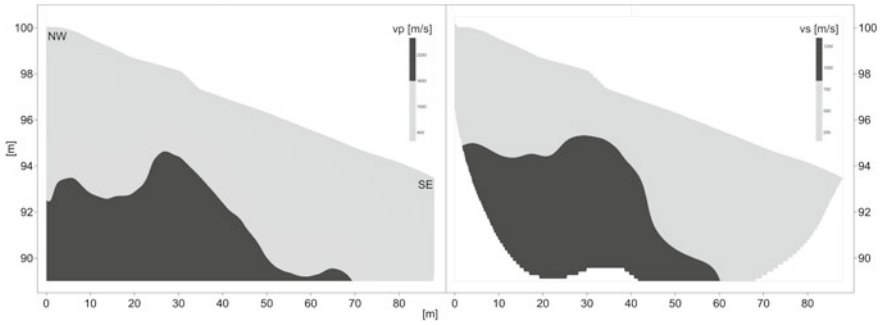


**Fig. 8.7** (*left*) P-wave model and (*right*) S-wave model as derived from tomographic inversion of first break traveltime picked in the data acquired using the hammer blow sources. These velocity models are used as an initial models for full-waveform inversion. Surface topography was taken into account in this inversion

sents a quaternary layer that covers the dark gray part which possibly shapes the bedrock surface consisting of sericite-gneiss. For P-waves a transition velocity of 1600 m/s is chosen whereas a velocity of 850 m/s illustrates the transition zone for the S-wave image. Even though the shape of the bedrock surface seems to vary inconstantly on both sides of the assumed fault, the 2D structure of the subsurface velocity distribution is obvious.

## 8.6 The Ultrasonics and Microseismic Field Laboratory

On scales of centimeters to decimeters seismic investigations may be applied to non-destructive testing of structures made of natural stone or concrete for example facades, engineering structures, pavements or monuments. Alterations or flaws caused by weathering or repeated usage may be detected by ultrasonic surface measurements along profiles of a length of up to about 30 cm using frequencies between about 5 and 500 kHz. In order to investigate the entire waveform a definite radiation pattern of the transducer and receiver and highly accurate point measurements are needed. In the framework of the project ultrasonic measuring devices well suited for reproducible surface measurements have been developed together with the project partner GEOTRON Elektronik. The equipment is easy to handle allowing for efficient and broadband measurements. Comparison of measured ultrasonic waveforms with synthetics calculated by numerical forward modeling shows that the source may be well approximated by a vertical point force and the receiver record essentially the vertical component of the wavefield (Mosca et al. submitted).

**Laboratory experiments.** Ultrasonic measurements were carried out before and after two phases of artificial weathering of samples made of natural stones and concrete in order to quantify the effect of weathering on velocities and damping of elastic

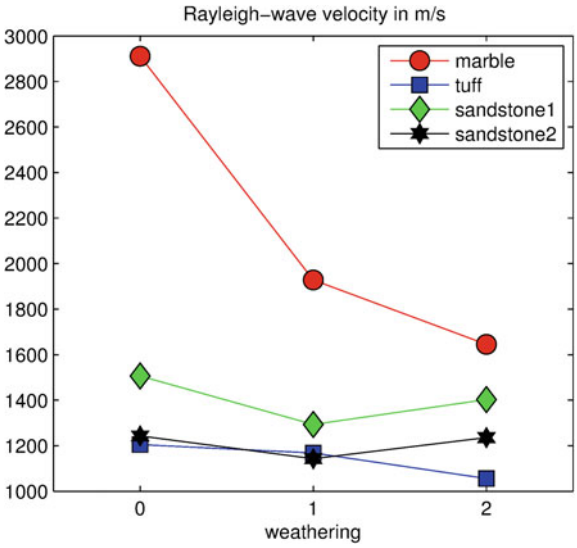


**Fig. 8.8** Average Rayleigh wave velocities in natural stones before and after two phases of weathering

waves. In addition, 4 samples of concrete made of different recipes were investigated. Figure 8.8 shows the results for Rayleigh wave velocities measured at the surface of the natural stone samples. From the figures it is obvious that weathering of natural stones may results in significant changes in average Rayleigh wave velocities. Interestingly, elastic velocities in marble decrease strongly already after the first phase of weathering and reduce by about 50 % after the second phase. Also in tuff the velocities are constantly decreasing in total by about 12 %. The behaviour of sandstones differs. After the first phase a decrease of the elastic velocities is observed whereas after the second phase they are increasing again. Very likely this is due to a decrease of porosity by filling of the pore space by clay and sand particles. In contrast, velocities in the concrete samples decrease strongly and monotonously due to weathering.

**Field experiments.** A number of measurements at real structures have been carried out—more than originally anticipated. Columns made of sandstone were measured at the *Klosterkirche Enkenbach-Alsenborn*. At the *Schlossbrücke, Berlin,* surface measurements were carried out at the the statue "Nike bekränzt den Sieger" made of Carrara marble. Roman plaster was investigated at the *Amphitheater Trier,* in the Vomitorium 3 (a former exit). A large number of measurements at different types of damage were carried out at the *Porta Nigra, Trier.* This Roman building is made of sandstone. It is famous for its black crust that is the result of weathering. At the *Tabularium at Campidoglio, Rome,* made of tuff alterations due to weathering were investigated. Roman plaster in the "House of the Tragic Poet" in *Pompei* was investigated by ultrasonic surface measurements. Finally, at a parking lot of the highway A4 the concrete pavement and a pillar of a bridge crossing the highway A9 were investigated. In all cases accurate and repeatable measurements of ultrasonic

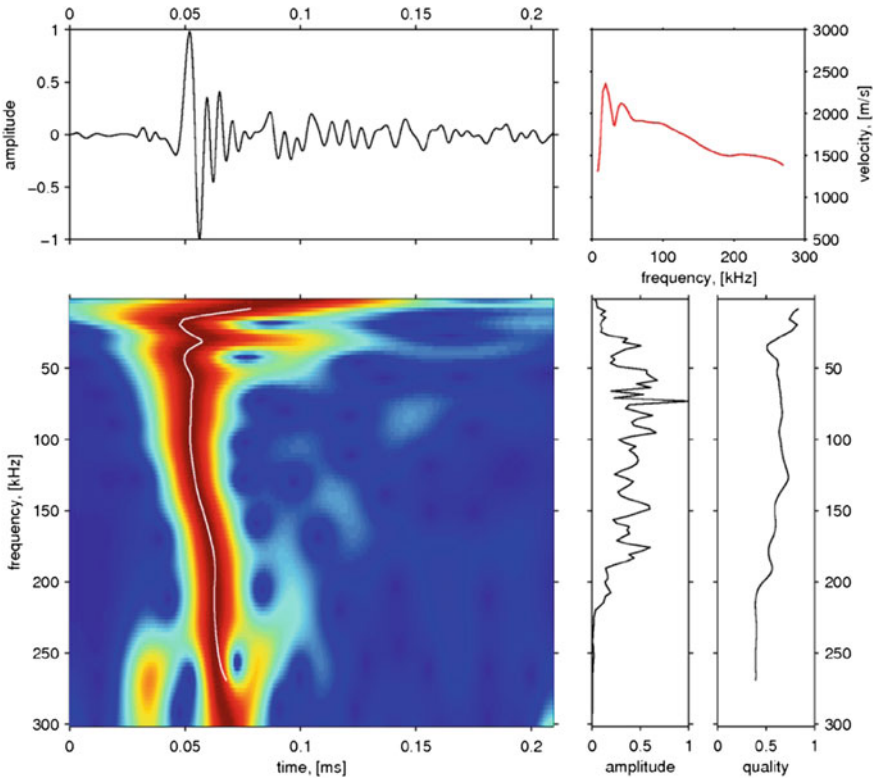


**Fig. 8.9** Spectrogram of a waveform measured at Klosterkirche Enkenbach-Alsenborn. (*top left*) Waveform recorded at 12 cm source-receiver distance. (*bottom left*) time-frequency analysis. *Red colors* indicate high amplitudes. The *white line* indicates the group travel time of the fundamental Rayleigh mode (*top right*) Group velocity of the fundamental Rayleigh mode. Note the decrease with increasing frequency pointing to superficial softening

waveforms have been obtained. They showed convincingly the potential of surface waveform measurements for the investigation of media properties in the uppermost centimeters. In all cases the waveforms of the Rayleigh fundamental mode are indicative for the changes of media properties with depth. In most of the cases, the velocity is slightly to strongly increasing with depth (Fig. 8.9). In some cases a high velocity crust of altered material has been found. This is e.g. typical for the intact black crust at the Porta Nigra or the Tabularium in Rome. Interestingly, pavement exposed to frequent mechanical load by cars and pillars affected by salty water in winter times showed slightly increased velocities.

**Software tools.** Various tools for the analysis of ultrasonic waveforms have been developed. This includes tools for the visualization of the waveforms and the determination of wave velocities for waves traveling along the profile. Time-frequency analysis for the determination of Rayleigh wave group velocities (Meier et al. 2004) was adapted to ultrasonic frequencies. This tool proved to be very useful

for the characterization of the waveforms and the detection of superficial changes in material properties. Furthermore, a tool for the linearized full-waveform inversion of ultrasonic surface measurements has been developed. Ultrasonic waveforms are calculated using the Gemini software package (Friederich and Dalkolmo 1995). Waveforms and Rayleigh wave group velocities may be inverted for a 1D model of the uppermost centimeters. The short computation time of only a few minutes on a standard PC ensures the effective applicability to real measurements.

## 8.7 Toolbox Management

One principal aim of TOAST is the dissemination of software products with all licensing questions resolved. Due to the open and collaborative nature in academics the TOAST toolbox pursues an open-source policy. For distribution the TOAST toolbox bundles components into packages which accomplish both simplicity and flexibility. In the following we describe important licensing issues that were discussed between the TOAST partners and are of broader relevance for open source software distribution projects.

### *8.7.1 Software Licensing*

Licensing is an important tool for setting specific terms on which software may be used, modified or distributed. By mistake, scientists often do not pay much attention to copyright and licensing issues. Making developments available for others is part and parcel in science. In particular, this holds true for reproducibility and the ability to build upon others' work. In fulfilling expectations to distribute and disseminate TOAST related software products appropriate licensing is mandatory. Otherwise exclusive rights are granted to the original work which potentially constitutes copyright infringements.

Software licenses can generally be fit into two categories: Proprietary software or closed source software and free-libre and open source software (FLOSS). Roughly spoken, proprietary licenses are designed with the intent to impose restrictions for modification, sharing, studying or redistribution. Thus, in the following, proprietary licenses are left out. FLOSS on the contrary means liberally licensing to grant users the right to use, copy, study, change, and improve its design through the availability of source code. Because of their open and non-discriminatory nature, FLOSS licenses can simplify development and collaboration which are driving forces in science.

There is a wide variety of liberal licenses which all share the ideas of *open source* and *free software*. Nevertheless, terms and conditions may differ significantly in certain respects and someone should precisely reflect which FLOSS license to choose. In doubt a lawyer should be consulted. The following gives a short introduction to terminology and some selected features often used to describe FLOSS licenses.

**Copyleft** is a concept to use copyright law to render any modified or extended versions to be considered *free* as well (e.g. GPL).

**Share-Alike** describes a license which requires any copy or adaptation to be released under the same or a very similar license as the original.

**Permissive** licenses are a class with minimal requirements on how the software can be redistributed. This is in contrast to *copyleft* and *share-alike*. Examples are MIT and BSD licenses.

**Compatible** licenses do not contain contradictory requirements which render it impossible to combine projects. For example, including BSD or MIT licensed code into a GPL project is possible but not vice versa.

**Linking** permissions allow to use and integrate code or libraries into a project without requiring to release the projects entire source code.

**Proliferation** of FLOSS licenses makes it difficult to choose a particular one coming along with increasing the chance of compatibility issues.

An often used FLOSS license is the GNU General Public License (GPL). If the ideas of *copyleft* and *share-alike* are appealing to a project it is a good choice. The majority of TOAST related software is published under the GPL.

### *8.7.2 Copyright Assignment*

When more than one person is involved or for collaborative and derived works copyright assignment has to be resolved. However, in many jurisdictions copyright can not be transfered i.e. the authorship is not negotiable. In general copyright assignment is a difficult field. A lawyer from the institute's legal department should assist. In case all contribution's and component's licenses are suitable and compatible then there is no reason not to publish under that very license. Broadly spoken, it is the easiest way to agree on the same license for any ingredient throughout the whole package, if possible. Otherwise, it is usually sufficient to collect—what is called—contributor license agreements (CLA). By complying with the CLA each person who works on a project explicitly grants the right to incorporate its contributions.

### *8.7.3 Software Packaging*

Besides licensing, it is very important to distribute scientific codes in a convenient way. From the viewpoint of users the software's usability is a key feature which also concerns the build- and installation process. Most scientists expect programs to run within an hour on commonly used systems. Accordingly, software should be provided as a package.

Providing bare but appropriate licensed source-code is not sufficient for most users. Packaging scientific code must be a trade-off between source-code only and all-round carefree installers. However, for distributing codes non-computer scientists do not want to break down system or software barriers.

As a compromise, for dissemination it is recommended to provide a single tar-archive which includes any ingredient necessary. The following list proposes what a resulting program package should contain. While those guidelines should not be ignored, they are not entirely put into practice by any TOAST related software-suite. To give an example, it depends on the actual project whether a toy-example is included or not.

**Source Code:** Each package must bring its sources along with any ingredient which is typically not available on the desired system.

**License:** Every single component in the package as source-code, documentation, examples have to be licensed properly. This also includes code snippets e.g. taken from textbooks.

**Readme:** By convention, this is the first file users will read. It should provide a first overview on what is contained and whom to ask.

**Documentation:** It is absolutely inevitable to provide proper and entire documentation on how the program has to be used.

**Build Guide:** Detailed instructions on how to build executables along with library or software prerequisites should be given.

**Version:** A widely used naming convention is to start with a stem prefix, followed by a dash followed by a version number.

**Build System:** To enable users compiling the code it is highly recommended having a *Makefile* to transform sources into executables.

**Getting Started:** To unburden first steps, a very concise tutorial should be include which might be wrapped around an example.

### *8.7.4 The OpenTOAST Initiative*

Throughout the funding period the TOAST project was mentoring various software projects. It was one of the key objectives to monitor and maintain the development process of software suits. As a result a collection of application has been taken together in what is called the TOAST-Toolbox. Codes to be considered have at least to comply with proper licensing and packaging guidelines put in to practice. In fact, actual software packages are made available through the TOAST partners. To provide an overview some selected core applications are listed in Table 8.1.

To preserve TOAST's current status and to offer an open and collaborative platform for applied seismic tomography a successor initiative beyond TOAST's funding period was formed. It is called the *OpenTOAST Initiative* (OTI). It pursues the goal to make actual implementations available throughout a wide academic community as well as end-users. It is OTI's commitment to share not only source code but also software, knowledge, contacts, and data. For further details please visit www.opentoast.de.

**Table 8.1** Selected core-applications covered by TOAST with all licensing question resolved, bundled into packages including documentation, build instructions and examples

| Name | Description | License |
|---|---|---|
| SOFI2D and SOFI3D | A massively parallel finite differences code for modeling 2D and 3D viscoelastic wave propagation in the time domain | GPLv2 |
| Gemini | Software suit to calculate Green's functions for the elastic wave equation in 1D media | GPLv2 |
| TFSoftware | A collection of tools to process, analyze and asses seismic wavefortn data | Mostly GPL |
| 3DFWI | Finite difference time-frequency doniain 3D elastic full-waveform inversion code using the adjoint method | GPLv2 |
| DENISE | Finite difference time domain 2D elastic full-waveform inversion code using the adjoint method | GPLv2 |
| FW-NA | Framework for probabilistic 1D full-waveform inversion based on neighborhood-algorithm | Proprietary and GPL |
| SES3D-NT | MPI parallelized 3D waveform modeling code in spherical coordinates covering itnaging capabilities | GPLv3+ |
| ASKI | A higlily modularized program suite for sensitivity analysis and iterative full-waveform inversion | GPLv2 |

**Acknowledgments** The project TOAST was funded by the German Federal Ministry of Education and Research (BMBF) within the R&D programme GEOTECHNOLOGIEN (Grant: 03G0752A-F).

## References

Bohlen T (2002) Parallel 3-D viscoelastic finite difference seismic modeling. Comput Geosci 28:887–889

Butzer S, Kurzmann A, Bohlen T (2013) 3D elastic full-waveform inversion of small-scale heterogeneities in transmission geometry. Geophys Prospect 61(6):1238–1251. doi:10.1111/1365-2478.12065

Forbriger T, Groos L, Schäfer M (in review) Line-source simulation for shallow-seismic data. Part 1: Theoretical background. Geophys J Int

Friederich W, Dalkolmo J (1995) Complete synthetic seismograms for a spherically symmetric earth by a numerical computation of Green's function in the frequency domain. Geophys J Int 122:537–550

Groos L (2013) 2D Full-waveform inversion of shallow-seismic Rayleigh waves. Dissertation, Karlsruhe Institute of Technology (KIT)

Groos L, Schäfer M, Forbriger T, Bohlen T (in review) 2D elastic full-waveform inversion of shallow-seismic Rayleigh waves in the presence of attenuation. Geophysics

Köhn D (2011) Time domain 2D elastic full-waveform tomography. Dissertation, Christian-Albrechts-Universität zu Kiel

Krauss F, Giese R, Alexandrakis C, Buske S (submitted) Seismic travel-time and attenuation tomography to characterize the excavation damaged zone and the surrounding rock mass of a newly excavated ramp and chamber. Int J Rock Mech Min Sci

Kurzmann, A. (2012) Applications of 2D and 3D full-waveform tomography in acoustic and viscoacoustic complex media. Dissertation, Karlsruhe Institute of Technology (KIT)

Kurzmann A, Przebindowska A, Köhn D, Bohlen T (2013) Acoustic full-waveform tomography in the presence of attenuation: a sensitivity analysis. Geophys J Int 195(2):985–1000. doi:10.1093/gji/ggt305

Meier T, Dietrich K, Stoeckhert B, Hajes H P (2004) 1-dimensional models of the shear-wave velocity for the eastern Mediterranean obtained from the inversion of Rayleigh wave phase velocities and tectonic implications. Geophys J Int 156:45–58

Mora M (1987) Nonlinear two-dimensional elastic inversion of multioffset data. Geophysics 52(9):1211–1228

Mosca I, Meier, T, Sigloch K (submitted) Ultrasonic surface wave propagation in multi-layered structures. Geophys J Int

Przebindowska A. (2013) Acoustic full-waveform inversion of marine reflection seismic data. Dissertation, Karlsruhe Institute of Technology (KIT)

Sambridge M. (1999a) Geophysical inversion with a neighbourhood algorithms I- searching a parameter space. Geophys J Int 138:479–494

Sambridge M (1999b) Geophysical inversion with a neighbourhood algorithms II- appraising the ensemble. Geophys J Int 138:727–746

Schäfer M, Groos L, Forbriger T, Bohlen T (in review) Line-source simulation for shallow-seismic data. Part 2: Full-waveform inversion - a 2D case study. Geophys J Int

Sirgue L, Etgen J, Albertin U (2008) 3D frequency domain waveform inversion using time domain finite difference methods. In: Extended Abstracts, 70th EAGE meeting. Rome, Italy, F022

Sirgue L, Pratt RG (2004) Efficient waveform inversion and imaging: a strategy for selecting temporal frequencies. Geophysics 69(1):231–248

Tarantola A (1988) Theoretical background for the inversion of seismic waveforms, including elasticity and attenuation. Pure Appl Geophys 128(1/2):365–399

Tromp J, Komatitsch D, Liu Q (2008) Spectral-element and adjoint methods in seismology. Commun Comput Phys 3(1):1–32

Zelt CA, Barton PJ (1998) 3D seismic refraction tomography: a comparison of two methods applied to data from the Faeroe Basin. J Geophys Res 103:7187–7210